

# Preparation of Porous and Nonporous Silica Nanofilms from Aqueous Sodium Silicate

Junhui He,<sup>†</sup> Shigenori Fujikawa,<sup>†</sup> Toyoki Kunitake,<sup>\*,†</sup> and Aiko Nakao<sup>‡</sup>

Frontier Research System and Surface Characterization Division, The Institute of Physical and Chemical Research (RIKEN), Hirosawa 2-1, Wako-shi, Saitama, 351-0198 Japan

Received April 10, 2003. Revised Manuscript Received June 6, 2003

Ultrathin SiO<sub>2</sub> films in the range of 2–50-nm thickness were readily fabricated from inexpensive sodium silicate as starting material by its alternate adsorption with cationic polymer and subsequent treatment with O<sub>2</sub> plasma and calcination. Film thickness can be controlled by adjusting the number of adsorption cycles and the pH value of silicate solution. Film surface is generally smooth (small roughness) and remains unchanged after O<sub>2</sub> plasma treatment or calcination. Whereas a nanoporous thin film is obtained by O<sub>2</sub> plasma treatment, a dense silica film is produced through calcination at 450 °C. These preparative methods prove that inexpensive sodium silicates are converted to advanced silica-based materials, such as functional ultrathin films, coatings, capsules, and catalysts, by simple procedures.

## Introduction

Ultrathin silica films have been attracting much attention because of their central roles in silicon technology and other important applications. For example, their high resistance to permeation of oxygen and water molecules makes them well suited as transparent barriers against oxygen and moisture in food packaging.<sup>1</sup> They are also effective as protective films of easily corroded materials such as metals, and silicon oxide layers are deposited on SnO<sub>2</sub> conductivity sensors to improve their selectivity and stability.<sup>2</sup> Scratch-resistant coatings for polymeric optical devices, such as polycarbonate optical lenses, is yet another example of the use of silicon oxide layers. They are also useful in microelectronics as intermetal dielectrics in interconnections and gate oxides in amorphous silicon transistors.<sup>3–5</sup> Inexpensive, flexible, and low-temperature processes are still strongly desired for formation of ultrathin silicon oxide layers of tailorable structures and properties in all these applications.

Several methods have been used to form ultrathin silicon oxide layers. One direct method is to heat a silicon wafer in air at a temperature over 1000 °C, forming a thin oxide layer on its surface. On other substrates, silicon oxide layers could be produced using spin-coating of silicon alkoxides and polysiloxanes, followed by UV-assisted removal of the organic components.<sup>3,4,6</sup> Photochemical vapor deposition (photo-CVD)

with silicon tetraacetate as the raw material has been used as well.<sup>7</sup> Kalachev et al.<sup>8</sup> and Mirley et al.<sup>9</sup> reported formation of silicon oxide layers by treatment of Langmuir–Blodgett films with low temperature plasma and UV/ozone. More recently, self-assembly processes were employed to fabricate silicon-containing inorganic/organic composite films from combinations of linear polycation with colloidal montmorillonite<sup>10</sup> or silica beads,<sup>11</sup> or from combination of oligosilsesquioxane and linear polyanion.<sup>12</sup> Subsequent calcination of the latter yielded silica films. It is strange that sodium silicate, a common, inexpensive material consisting of linear, branched, and ring-shaped oligomers, has not been used as a precursor of silicon oxide films. We recently demonstrated that low-temperature O<sub>2</sub> plasma effectively removed the organic component from hybrid molecular multilayers of poly(acrylic acid) and titania gel.<sup>13</sup> A similar approach may be applicable to preparation of silicon oxide layers from sodium silicate. In the present work, we report fabrication of nano-hybrid films of sodium silicate and polycation (PDDA) via electrostatic self-assembly and their conversion to silicon oxide films via low-temperature O<sub>2</sub> plasma and thermal treatments.

## Experimental Section

**Materials.** Poly(diallyldimethylammonium chloride) (PDDA, MW 240 000, 20% solids) and poly(acrylic acid) (PAA,  $M_n$

\* To whom correspondence should be addressed. E-mail: kunitake@ruby.ocn.ne.jp.

<sup>†</sup> Frontier Research System.

<sup>‡</sup> Surface Characterization Division.

(1) Rotger, J. C.; Pireaux, J. J.; Caudano, R.; Thorne, N. A.; Dunlop, H. M.; Benmalek, M. *J. Vac. Sci. Technol. A* **1995**, *260*.

(2) Althainz, P.; Dahlke, A.; Goschnick, J.; Ache, H. *J. Thin Solid Films* **1994**, *241*, 344.

(3) Niwano, M.; Kinashi, K.; Saito, K.; Miyamoto, N.; Honma, K. *J. Electrochem. Soc.* **1994**, *141*, 1556.

(4) Joubert, O.; Hollinger, G.; Fiori, C.; Devine, R. A. B.; Paniez, P.; Pantel, R. *J. Appl. Phys.* **1991**, *69*, 6647.

(5) Klumpp, A.; Sigmund, H. *Appl. Surf. Sci.* **1989**, *43*, 301.

(6) Ouyang, M.; Yuan, C.; Muisener, R. J.; Boulares, A.; Koberstein, J. T. *Chem. Mater.* **2000**, *12*, 1591.

(7) Maruyama, T.; Tago, T. *Thin Solid Films* **1993**, *232*, 201.

(8) Kalachev, A. A.; Mathauer, K.; Hoehne, U.; Moehwald, H.; Wegner, G. *Thin Solid Films* **1993**, *228*, 307.

(9) Mirley, C. L.; Koberstein, J. T. *Langmuir* **1995**, *11*, 1049.

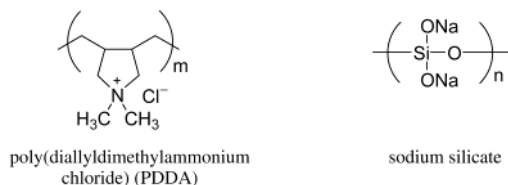
(10) Lvov, Y.; Ariga, K.; Ichinose, I.; Kunitake, T. *Langmuir* **1996**, *12*, 3038.

(11) Lvov, Y.; Ariga, K.; Onda, M.; Ichinose, I.; Kunitake, T. *Langmuir* **1997**, *13*, 6195.

(12) Cassagneau, T.; Caruso, F. *J. Am. Chem. Soc.* **2002**, *124*, 8172.

(13) (a) Huang, J.; Ichinose, I.; Kunitake, T.; Nakao, A. *Nano Lett.* **2002**, *2*, 669; (b) Huang, J.; Ichinose, I.; Kunitake, T.; Nakao, A. *Langmuir* **2002**, *18*, 9048.

Chart 1



11 700,  $M_w/M_n$  1.07) were purchased from Polysciences and Polymer Source, respectively. Aqueous sodium silicate ( $\text{SiO}_2$  35–38%), 3-mercaptopropionic acid and hydrochloric acid (35.0–37.0%) were obtained from Kanto Chemical. All these chemicals were used as purchased. Ultrapure water with a specific resistance of 18.3  $\text{M}\Omega\cdot\text{cm}$  was obtained by reverse osmosis followed by ion-exchange and filtration (Yamato-WQ500, Millipore). The pH of aqueous sodium silicate was adjusted by adding hydrochloric acid.

**Quartz Crystal Microbalance.** A quartz crystal microbalance (QCM, 9 MHz) device manufactured by USI System, Fukuoka, was used for monitoring layer-by-layer film assembly and removal of organic components. Gold-coated QCM resonators were treated with Piranha solution (96.0% sulfuric acid/30.0–35.5% hydrogen peroxide, 3:1, v/v), rinsed with pure water, and dried by flushing with nitrogen gas. They were then immersed in an ethanol solution of 3-mercaptopropionic acid (10 mM) for 12 h, followed by rinsing with ethanol and drying with nitrogen gas. Stable frequency shifts due to layer-by-layer adsorption cycles and plasma etching of organic components were recorded in air after drying and transformed into mass changes by using the Sauerbrey equation.<sup>14</sup> In our system, a frequency decrease of 1 Hz corresponds to a mass increase of 0.87 ng. The thickness of adsorbed layers ( $d$ ) on one side of the QCM resonator is given by

$$d(\text{nm}) = 0.027 (-\Delta F(\text{Hz}))/\rho \quad (1)$$

where  $\rho$  is the density of adsorbed material: 2.61  $\text{g}/\text{cm}^3$  for sodium silicate and 1.2  $\text{g}/\text{cm}^3$  for the polyelectrolyte.<sup>10</sup>

**Preparation of Ultrathin Silicon Oxide Films.** In a typical example, precursor layers of (PDDA/PAA)<sub>3</sub> were assembled by alternate immersion (3 cycles) of a 3-mercaptopropionic acid-modified electrode in aqueous PDDA (10 mg/mL, pH 7) and in ethanolic PAA (10 mg/mL) at room temperature for 10 min, followed by rinsing with pure water for 1 min and drying with nitrogen gas. Then, PDDA and silicon oxide layers were built up alternately on the precursor film by using aqueous PDDA (10 mg/mL) and aqueous sodium silicate (100 mM) in the same way. At the end of each adsorption procedure, the electrode was attached to a QCM frequency counter and a stable frequency was recorded after rinsing the electrode with pure water and drying it with nitrogen gas. Such PDDA/silicon oxide composite films were directly deposited on the silicon wafer without deposition of the (PDDA/PAA)<sub>3</sub> precursor film.

The inorganic/organic composite films were subjected to low-temperature  $\text{O}_2$  plasma treatment or calcination, thus their organic components being removed to give ultrathin silicon oxide films.  $\text{O}_2$  plasma treatment was carried out on a PE-2000 Plasma Etcher (South Bay Technology). A pressure-regulated flow rate of 0.06 MPa was set on the  $\text{O}_2$  gas cylinder. The plasma chamber was evacuated to ca. 80 mTorr before introduction of  $\text{O}_2$  gas. The operating pressure was regulated at ca. 180 mTorr. The forward power was set at 30 w, while the reflected power was optimized. Calcination was carried out in a programmable KDF-S70 furnace manufactured by Denken, Japan. The samples were heated at a rate of 17.2  $^\circ\text{C}\cdot\text{min}^{-1}$  to 450  $^\circ\text{C}$ , kept at this temperature for 4 h, and then allowed to cool to room temperature.

**Scanning Electron Microscopy (SEM) and Atomic Force Microscopy (AFM).** The films on QCM electrodes were cleaved, and 2 nm of Pt was coated on them with a Hitachi

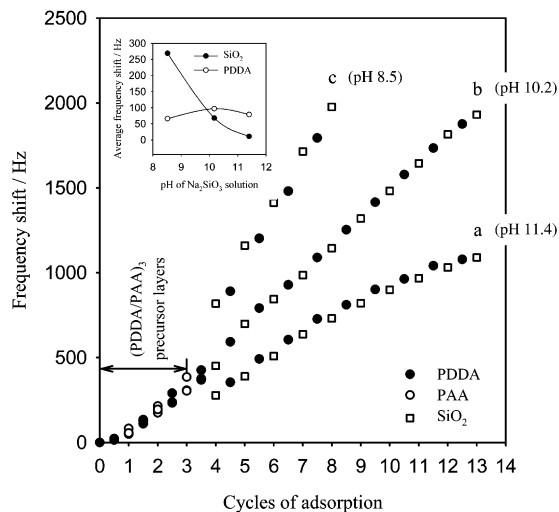


**Figure 1.** Alternate deposition of aqueous PDDA (pH 7.0) and aqueous sodium silicate of pH 11.4 (a), 10.2 (b), and 8.5 (c). Insert: pH dependence of average frequency shifts of PDDA and  $\text{SiO}_2$  layers. Aqueous PDDA (10 mg/mL), PAA (10 mg/mL in ethanol), and aqueous sodium silicate (100 mM). The concentrations used in other figures are identical.

E-1030 ion-coater. Then the films were observed on a Hitachi S-900 scanning electron microscope. The films assembled on silicon wafer were directly observed on a Hitachi S-5200 field emission scanning electron microscope (FE-SEM) without any coating. Atomic force microscopy (AFM) measurements were carried out by noncontact mode on an Explorer Scanning Probe Microscope TMX2100 (TopoMetrix).

**FT-IR Measurements and X-ray Photoelectron Spectroscopy (XPS).** For FT-IR measurements, films of (PDDA/PAA)<sub>3</sub>(PDDA/ $\text{SiO}_2$ )<sub>20</sub> were assembled on a piece of 3-mercaptopropionic acid-modified gold-coated micro glass (25 × 9 mm<sup>2</sup>, Thermo Spectra-Tech gold coated microscope slide). Their IR spectra were collected before and after calcination at 450  $^\circ\text{C}$  for 4 h on a NEXUS 670 FT-IR unit (Thermo Nicolet) by subtracting the substrate absorption as the background. Ultrathin films of (PDDA/ $\text{SiO}_2$ )<sub>5</sub> were also assembled on silicon wafer substrates, and XPS spectra were measured on an ESCALAB 250 (VG) using Al K $\alpha$  (1486.6 eV) radiation before and after  $\text{O}_2$  plasma treatment or calcination. The applied power was operated at 15 kV and 20 mA. The base pressure in the analysis chamber was less than  $10^{-8}$  Pa. Smoothing, background removal, and peak fitting were carried out with a VG analysis software package, ECLIPS. All the peaks were corrected with C 1s (285 eV) as the reference.

## Results and Discussion

**Assembly of Ultrathin PDDA/ $\text{SiO}_2$  Composite Films.** PDDA has been used frequently as a linear polycation for electrostatic alternate assembly. In contrast, sodium silicate has not been used in electrostatic assembly. It is often represented by a linearly condensed structure, but its more plausible structure appears to be a mixture of linear, branched, and ring-shaped oligomers. Its composition depends on the pH value of the solution.<sup>15</sup>

Figure 1 shows the film assembly process from aqueous PDDA and sodium silicate, as monitored by QCM. The first three cycles of adsorption represent formation of the (PDDA/PAA)<sub>3</sub> precursor film with the outermost negative PAA layer. Subsequently, PDDA/

(14) Sauerbrey, G. Z. Phys. 1959, 155, 206.

(15) Trotman-Dickenson, A. F., Ed. *Comprehensive Inorganic Chemistry*, 1st ed.; Compendium Publishers: Elmsford, NY, 1973; Vol. 1, p 1413.

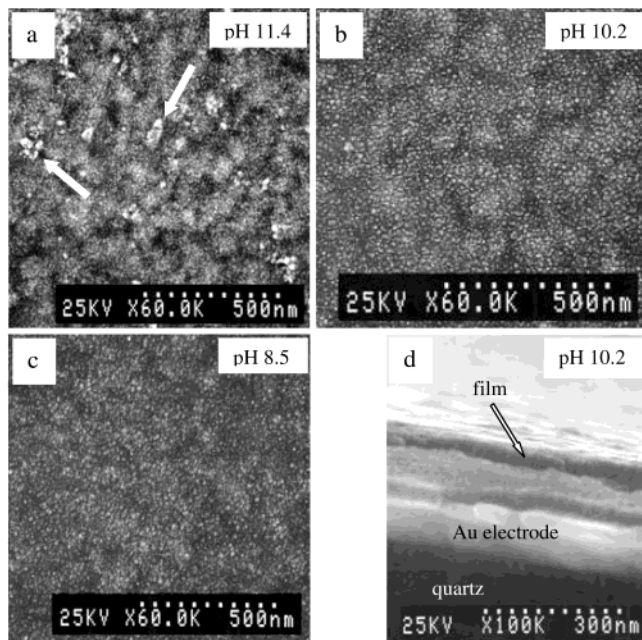


**Figure 2.** SEM top views of the films fabricated at pH 11.4 (a), 10.2 (b), and 8.5 (c) of aqueous sodium silicate and cross-sectional view (d). Arrows in (a) point to sodium silicate aggregates.

SiO<sub>2</sub> composite films were assembled by alternate adsorption of PDDA and sodium silicate. Linear frequency shifts indicate that regular film growth was achieved. When the pH of aqueous sodium silicate is 11.4, the average frequency shift for silicate adsorption ( $\Delta F_{\text{SiO}_2}$ ) is only 11 Hz, while that for PDDA adsorption ( $\Delta F_{\text{PDDA}}$ ) is 79 Hz (Figure 1a).  $\Delta F_{\text{PDDA}}$  did not change extensively with pH of the silicate solution (97 Hz at pH 10.2, 66 Hz at pH 8.5), but  $\Delta F_{\text{SiO}_2}$  increased markedly with pH (68 Hz at pH 10.2, 269 Hz at pH 8.5); see insert of Figure 1. Aqueous silicate was stable at pH 10.2 and 11.4, but fresh silicate solutions had to be prepared for each adsorption at pH 8.5 due to gradual gelation with time. It is known that the molecular weight of silicate in water increases with decreasing pH values.<sup>15</sup> Thus, the enhanced frequency shift for silicate adsorption at lower pHs may be attributed to increased molecular weight of silicate oligomers.

The thickness of the alternate film (13 cycles) prepared at pH 10.2 (curve b in Figure 1) was estimated by eq 1 to be ca. 35 nm. In turn, the average density of this film was calculated to be 1.5 g/cm<sup>3</sup>, which is between those of PDDA and sodium silicate. The thicknesses of the films assembled at pH 11.4 and 8.5 (curves a and b) were estimated to be 25 and 28 nm, respectively.

Film morphology was examined by SEM. Figure 2 shows surface morphologies of the as-prepared film fabricated at different pH values of aqueous sodium silicate (Figure 1). The (PDDA/PAA)<sub>3</sub>(PDDA/SiO<sub>2</sub>)<sub>10</sub> film assembled at pH 11.4 (curve a in Figure 1) is covered with aggregates of sizes of 30–200 nm (indicated by arrows) (Figure 2a). At lower pH values (pH 10.2 and 8.5), however, such aggregates are not observed, and the film surfaces are quite smooth (Figure 2b and c). This morphology difference may be explained by the change of the adsorbed silicate species. The silicate anion exists as monomeric species at high pH, and is

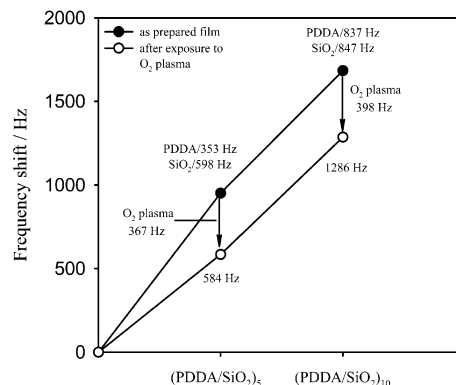


**Figure 3.** QCM frequency shifts of (PDDA/SiO<sub>2</sub>)<sub>5</sub> and (PDDA/SiO<sub>2</sub>)<sub>10</sub> films fabricated at pH 10.2 before (filled circles) and after (empty circles) O<sub>2</sub> plasma treatment at 30 W for 30 min.

converted to oligomeric species at lower pH. The monomeric species appear to produce 3D aggregates on the oppositely charged film surface. In contrast, oligomeric silicates will be more tightly bound to the surface, giving smooth films. Aqueous sodium silicate of pH 8.5 tends to gel gradually with time, thus, that of pH 10.2 was most suitable for film assembly. Figure 2d shows the cross-sectional view of the (PDDA/PAA)<sub>3</sub>(PDDA/SiO<sub>2</sub>)<sub>10</sub> film assembled at pH 10.2. The composite thin film, gold electrode, and quartz substrate are clearly seen. The thickness of the composite thin film is uniform and estimated to be ca. 35 nm, in good agreement with that estimated from QCM frequency shifts.

**Removal of Organic Components by Low-Temperature O<sub>2</sub> Plasma and Calcination.** O<sub>2</sub> Plasma treatment and calcination were used to remove organic moieties in the film. The O<sub>2</sub> plasma treatment was carried out at 30 W first for 30 min on a PE-2000 Plasma Etcher. The process was monitored by QCM and the results are shown in Figure 3. In the preparation of a (PDDA/SiO<sub>2</sub>)<sub>5</sub> film, 5 layers of PDDA corresponded to a frequency shift of 353 Hz and 5 layers of SiO<sub>2</sub> corresponded to a frequency shift of 598 Hz. The total frequency shift (PDDA + SiO<sub>2</sub>) was 951 Hz. Exposure of this film to O<sub>2</sub> plasma for 30 min gave a frequency increase of 367 Hz, corresponding to removal of the whole PDDA component (353 Hz). Further O<sub>2</sub> plasma treatment did not lead to any frequency shift. The remaining frequency shift (951 Hz – 367 Hz = 584 Hz) was very close to that of 5 layers of SiO<sub>2</sub> (598 Hz). Thus the (PDDA/SiO<sub>2</sub>)<sub>5</sub> composite film became a SiO<sub>2</sub> thin film after O<sub>2</sub> plasma treatment. To test the depth of penetration of O<sub>2</sub> plasma, the (PDDA/SiO<sub>2</sub>)<sub>10</sub> film was also exposed to O<sub>2</sub> plasma under the identical conditions. The film thickness corresponded to a frequency shift of 1684 Hz, in which 10 layers each of PDDA and SiO<sub>2</sub> corresponded to frequency shifts of 837 and 847 Hz, respectively. When this film was exposed to O<sub>2</sub> plasma for 30 min, a frequency increase of 398 Hz was recorded. This frequency shift is almost half of that of the total PDDA layers (837 Hz) and it must be caused by removal of the outer half of the PDDA layers. No further frequency shift was observed upon additional O<sub>2</sub> plasma treatment for another 30 min, suggesting that the underlying PDDA layers could not be removed. These data do not contradict one another; they indicate that the depth of O<sub>2</sub> plasma penetration is limited to the five cycles of adsorption.



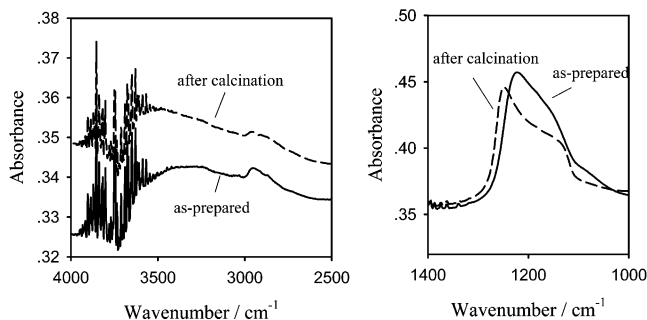


**Figure 4.** FT-IR spectra of as-prepared film ((PDDA/PAA)<sub>3</sub>-(PDDA/SiO<sub>2</sub>)<sub>20</sub>) and the same film after thermal treatment at 450 °C for 4 h.

Organic components are also removed from organic–silica composites by calcination at 450 °C for 4 h.<sup>16</sup> We have carried out calcination of the (PDDA/SiO<sub>2</sub>)<sub>10</sub> film in a programmable KDF-S70 furnace. Unfortunately, QCM measurement became unstable after calcination, probably due to deterioration of the electrode used. FT-IR technique was, therefore, used to monitor this calcination process. A sample of (PDDA/SiO<sub>2</sub>)<sub>20</sub> was assembled on a piece of gold-coated micro slide glass in order to obtain stronger IR signals. The spectra recorded before and after calcination are shown in Figure 4. Absorption in the range of 3050–2850 cm<sup>-1</sup> is attributed to the stretching vibrations of –CH<sub>3</sub> and –CH<sub>2</sub>– groups. A broad band at 3600 to 3000 cm<sup>-1</sup> is assigned to the stretching vibration of H<sub>2</sub>O, indicating that the film is hydrated. A peak at 1222 cm<sup>-1</sup> (longitudinal mode) and a shoulder (asymmetric stretching mode) at 1080 cm<sup>-1</sup> are typical of amorphous silicon oxide.<sup>17</sup> After calcination, however, the absorptions from H<sub>2</sub>O and organic components almost disappeared. The minor remaining absorption at 3000 to 2800 cm<sup>-1</sup> was probably due to contamination. In contrast, the intensities of the peaks of amorphous silicon oxide did not change much. It is noted that these peaks were shifted to higher wavenumbers upon calcination, indicating that the film became more like solid silica. Similar shifts were also reported for co-sputtered Si/SiO<sub>2</sub> layers<sup>17</sup> and for silicon-rich suboxide (SiO<sub>x</sub>,  $x < 2$ ) films deposited by plasma-enhanced CVD.<sup>18</sup>

The above results from QCM and FT-IR measurements are further supported by XPS data. As shown in Figure 5A, two large sharp peaks of Si 2p<sub>1/2</sub> (99.54 eV) and Si 2p<sub>3/2</sub> (98.94 eV) from atomic silicon (Si (0)), and a small broad peak of Si 2p (102.99 eV) from SiO<sub>2</sub> (Si (IV)) were observed for the silicon wafer substrate (curve a). The ratio of Si (0) to Si (IV) was estimated to be ca. 3.8:1. The small amount of SiO<sub>2</sub> detected was attributed to the oxidation of dangling bonds on the surface of the silicon wafer. When 5 cycles of PDDA/SiO<sub>2</sub> were assembled on the substrate, the Si (IV) peak was much enhanced, while the Si (0) peaks decreased (Figure 5A, curve b) due to coverage by the (PDDA/SiO<sub>2</sub>)<sub>5</sub> composite film. The ratio of Si (0) to Si (IV) was reversed (1:5.6). Meanwhile, a peak attributable to N 1s was observed

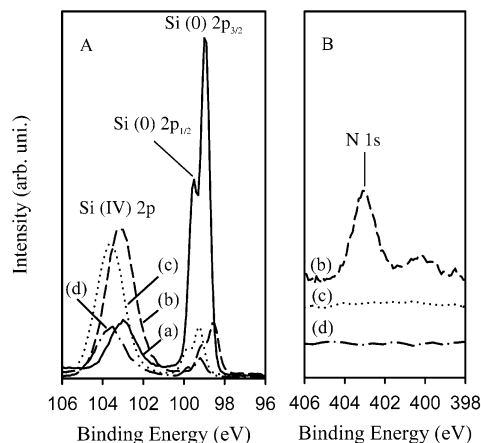


**Figure 5.** XPS spectra of silicon wafer (a) and (PDDA/SiO<sub>2</sub>) film assembled on it before (b) and after O<sub>2</sub> plasma treatment (c) and calcination (d).

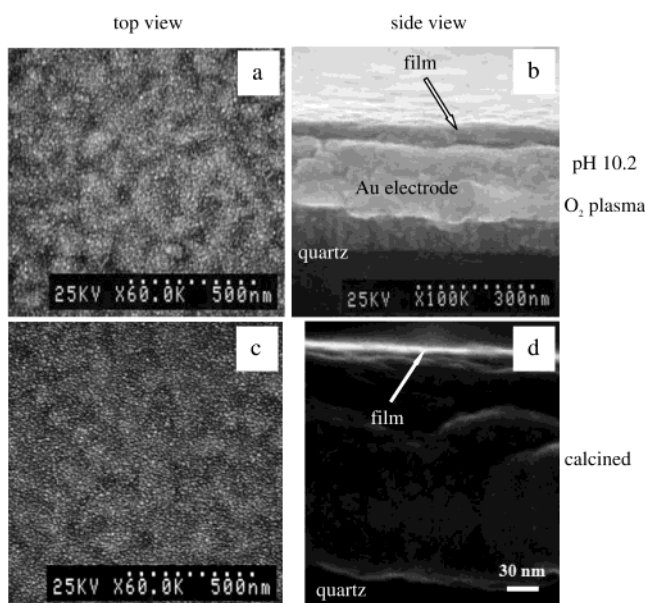


**Figure 6.** SEM top views and cross-sectional views of the film in Figure 2b after O<sub>2</sub> plasma treatment (at 30 W for 60 min) (a and b) and calcination (at 450 °C for 4 h) (c and d).

at 403.10 eV (Figure 5B, curve b). These facts indicate that PDDA and SiO<sub>2</sub> were effectively deposited on the substrate. After exposure to O<sub>2</sub> plasma and calcination, the N 1s peak completely disappeared (Figure 5B, curves c and d), while the ratio of Si (0) to Si (IV) remained almost unchanged (1:5.3 for the O<sub>2</sub> plasma treated film and 1:5.5 for the calcined sample, respectively). It is clear that PDDA was completely removed by O<sub>2</sub> plasma treatment and calcination, in agreement with the QCM (Figure 3) and FT-IR (Figure 4) results.

The morphologies of the films after removal of organic components by O<sub>2</sub> plasma (Figure 6a and b) and calcination (Figure 6c and d) were examined by using SEM and compared with that of the as-prepared composite film (Figure 2b and d). The top views indicate that the morphology of the film surface did not change much before and after the removal, i.e., smooth surfaces were obtained in all these cases (Figure 6a and c). In contrast, the side views show clear changes in film thickness. After exposure to O<sub>2</sub> plasma (30 W for 60 min), the thickness of the (PDDA/PAA)<sub>3</sub>(PDDA/SiO<sub>2</sub>)<sub>10</sub> film was enhanced to 42 nm (Figure 6b) from that of

(16) Velev, O. D.; Jede, T. A.; Lobo, R. F.; Lenhoff, A. M. *Nature* **1997**, *389*, 447.

(17) Charvet, S.; Madelon, R.; Rizk, R.; Garrido, B.; Gonzalez-Varona, O.; Lopez, M.; Perez-Rodriguez, A.; Morante, J. R. *J. Lumin.* **1999**, *80*, 241.

(18) Yun, F.; Hinds, B. J.; Hatatani, S.; Oda, S.; Zhao, Q. X.; Willander, M. *Thin Solid Films* **2000**, *375*, 137.

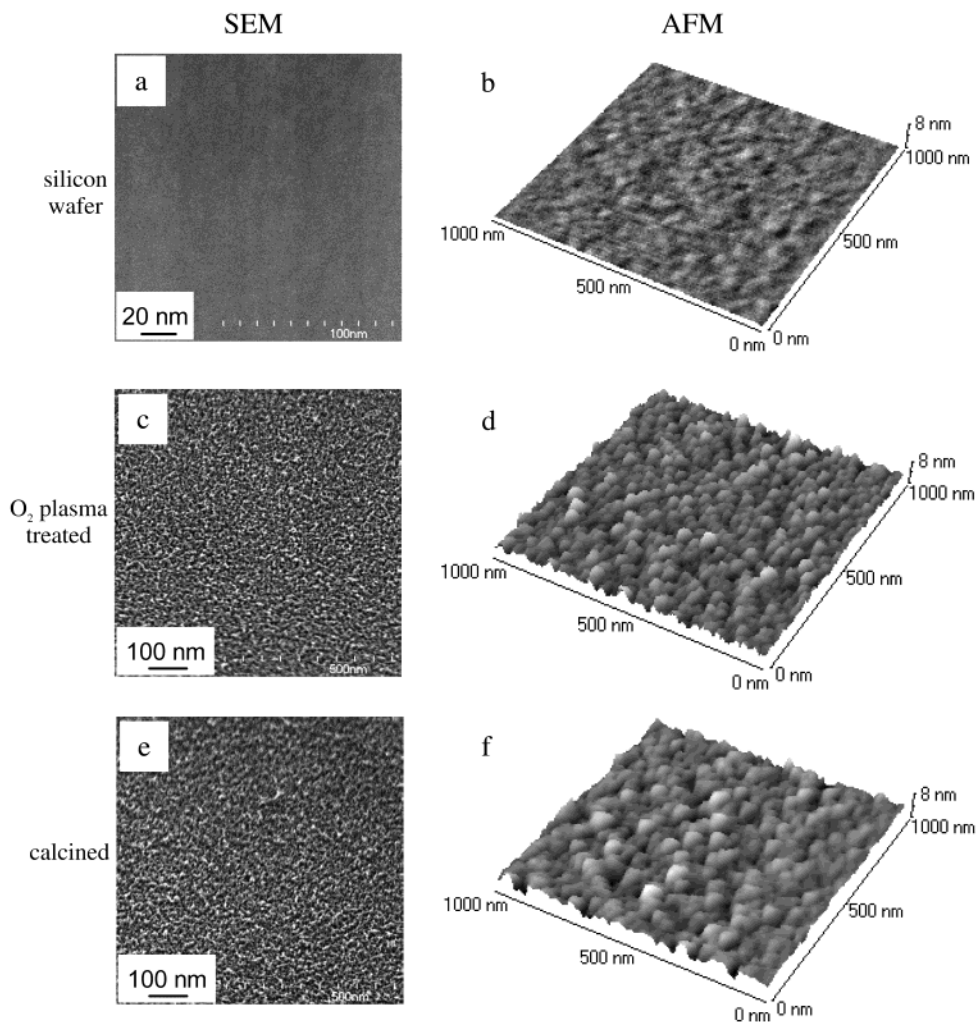


**Figure 7.** SEM (left) and AFM (right) images of surfaces of silicon wafer (a and b), and SiO<sub>2</sub> films obtained by O<sub>2</sub> plasma treatment (c and d) and by calcination (e and f).

the as-prepared film (35 nm) (Figure 2d). This represents a 20% increase in film thickness. From this film thickness and QCM frequency shift (1552 Hz after O<sub>2</sub> plasma treatment), the apparent film density was estimated to be 1.0 g/cm<sup>3</sup>. Such a density decrease and the resulting nanopore formation were previously observed in TiO<sub>2</sub>/PAA ultrathin films.<sup>13</sup> Removal of PDDA by O<sub>2</sub> plasma must have left nanovoids in the SiO<sub>2</sub> film, resulting in the decrease of apparent density. In contrast, when the as-prepared composite film was calcined at 450 °C for 4 h, the film thickness decreased to around 14 nm (Figure 6d), i.e., a 60% reduction from that of the as-prepared composite film. A similar change (50% decrease in film thickness) was reported by Ferguson et al. for a PDDA/titanium (hydr)oxide film.<sup>19</sup> The density of the obtained film was estimated to be 2.0 g/cm<sup>3</sup> according to eq 1, which is larger than that of the as-prepared film (1.5 g/cm<sup>3</sup>) and approaches that of silica (2.2–2.6 g/cm<sup>3</sup>). Thus, calcination produced a dense silica film. Such calcination-induced densification was similarly observed for TiO<sub>2</sub> films assembled by alternation of PDDA and titania nanosheet<sup>20</sup> or by the surface sol–gel process.<sup>21</sup>

**Fabrication of Ultrathin Silicon Oxide Films of Thickness Less Than 10 nm.** We further tested the

current approach for preparation of even thinner films by decreasing the number of alternate adsorption cycles. Two cycles of PDDA/SiO<sub>2</sub> were deposited on silicon wafer. The thickness of the as-prepared film was estimated to be ca. 6 nm from QCM results. After O<sub>2</sub> plasma treatment and calcination, the film thickness was expected to become ca. 7 nm and ca. 2 nm, respectively, based on the conclusions drawn from Figure 6. However, direct observation of their cross-sections by SEM was difficult. It is important to know whether the surface is fully covered by the deposited film. This was examined by comparing FE-SEM observation (without any coating) and AFM observation (Figure 7). Figure 7a is a SEM image of the extremely smooth surface of silicon wafer itself at a magnification of 500 000. Uniformly deposited layers are seen for the as-prepared film (not shown), and for those after O<sub>2</sub> plasma treatment (Figure 7c) and after calcination (Figure 7e).

Figure 7b, d, and f are AFM images of the silicon wafer substrate, and the films after O<sub>2</sub> plasma treatment and after calcination, respectively. The surface of the substrate itself was extremely smooth. The root-

(20) Sasaki, T.; Ebina, Y.; Fukuda, K.; Tanaka, T.; Harada, M.; Watanabe, M. *Chem. Mater.* **2002**, *14*, 3524.

(21) He, J.; Ichinose, I.; Fujikawa, S.; Kunitake, T.; Nakao, A. *Chem. Mater.* **2002**, *14*, 3493.

(19) Rouse, J. H.; Ferguson, G. S. *Adv. Mater.* **2002**, *14*, 151.

mean-square (RMS) roughness<sup>22</sup> was determined to be only 0.062 nm. It increased to 0.73 nm after deposition of (PDDA/SiO<sub>2</sub>)<sub>2</sub> (AFM image not shown), more than 10 times larger than that of the substrate. This indicated again that the (PDDA/SiO<sub>2</sub>)<sub>2</sub> film was effectively deposited on the surface of silicon wafer substrate. O<sub>2</sub> plasma treatment and calcination did not cause large changes in the surface morphology of the film (Figure 7d and f), in agreement with the FE-SEM observation. The RMS roughness remained to be 0.83–0.86 nm. Compared with the expected film thicknesses, i.e., 7 nm for the O<sub>2</sub> plasma treated film and 2 nm for the calcined film, closely packed islands might exist on the substrate surface after calcination. A closer look at Figure 7d and f reveals that the structural features are somewhat larger for the calcined film, suggesting that heat treatment might have caused fusion of smaller structures.

In summary, we have demonstrated a facile method of preparation of ultrathin SiO<sub>2</sub> films in the range of

---

(22) The root-mean-square (RMS) roughness,  $R_{\text{ms}} = \sqrt{1/N \sum_{i=1}^N (z_i - \bar{z})^2}$ .

2–50-nm thickness. Inexpensive sodium silicate was used as starting material, and alternate adsorption and posttreatments were combined. The prepared films are uniform before and after O<sub>2</sub> plasma treatment or calcination, and their thicknesses can be controlled by adjusting the number of adsorption cycles and the pH value of silicate solution. The surface morphology is generally smooth (small roughness) and remains unchanged after O<sub>2</sub> plasma treatment or calcination. Whereas a nanoporous thin film is obtained by O<sub>2</sub> plasma treatment, a denser film is produced through calcination at 450 °C. Such ultrathin films would be similarly deposited on curved surfaces of micro- and nano-objects, and are functionalized by incorporating functional units such as nanoparticles. Advanced silica-based materials such as functional ultrathin films, coatings, capsules, and catalysts could be prepared from inexpensive sodium silicate under energy-saving conditions.

CM034253D